© 2018 IJSRST | Volume 4 | Issue 8 | Print ISSN: 2395-6011 | Online ISSN: 2395-602X
Themed Section: Science and Technology

Detection and classification of combined real time power quality disturbance signals with Hidden Markov Models incorporating wavelet features

S. Upadhyaya
Department of Electrical Engineering, SUIIT, Burla, Sambalpur India

ABSTRACT

In this paper, Maximum Overlapping Discrete Wavelet Transform (MODWT) has been implemented along with the traditional discrete Wavelet Transform (DWT) for the detection and localization of different types of power quality (PQ) disturbance signals. Selected features have been extracted from the detail coefficient of the variants of WT and then fed as inputs to the classifiers in order to characterize the signals. Moreover, a comparative assessment of the PQ signal carried out with different classifiers such as Multilayer perceptron (MLP) and Hidden Markov Models (HMMs). Moreover, in order to represent in realistic environment, these proposed techniques are tested with signals captured from transmission line panels. Further, to aid this PQ disturbance detection, different types of real time fault signals are also characterized with these aforementioned approaches.

I. INTRODUCTION

The Power Quality disturbance (PQD) study has become an emerging issue in the area of power system, as the disturbances affect the overall harmony of the system. The proper and the continuous monitoring of the power quality disturbances has become a significant issue both for the utilities and the end-users. The operation of the power system can be improved by analyzing the PQ disturbances consistently. Hence, the development of the techniques and the methodologies in order to diagnose the power quality disturbances has acquired great importance in research. The PQ is actually the combination of quality of the voltage and the quality of current [1], [2] but in most of the cases, it is generous with the quality of voltage as the power system can only control the voltage quality. Hence, the yardstick of the power quality area is to preserve the supply voltage within the tolerable limits [3], [4]. The maintenance of quality of power in terms of voltage requires proper selection of the suitable detection and the characterisation methods. These are the crucial steps for maintenance of healthy power system by mitigating the PQ disturbances.

In order to identify the disturbances, the different techniques such as the Fourier transform (FT), the short-time Fourier transform (STFT), wavelet transform (WT), Neural Network, Fuzzy logic, S-transform have been used [5], [6]. The FT is a fast technique which only provides the information about the frequency component. So, FT is unsuitable for the analysis of non-stationary signal. On the other hand, the time frequency information related to the disturbance waveform can be obtained in STFT [7]. However, STFT is not suitable to track the transient signals perfectly due to its fixed window property [8]. Similarly, the S-transform suffers from computational burden which limits its applications [9]. The wavelet transform affords the timescale analysis of the non-stationary signal due to Multi-Resolution Analysis (MRA) property. The property of MRA of WT represents the signals into different time-scales rather than the time-frequency like the STFT. Thus, WT is a suitable technique for analysis of the transient signals as it provides long window at low frequencies and short window at high frequencies [10].

The automatic detection of PQ events with the discrete wavelet transform (DWT) is a common topic in past studies [11], [12]. But the DWT is restricted with the size of the signal. A modified version of DWT is known as maximal overlap discrete wavelet transform (MODWT) is adopted in this paper. The coefficients of the proposed method are not affected by changing the starting point and also has no restrictions on the size of signal unlike the traditional DWT. The MODWT has been implemented [13], [14] as 'undecimated DWT' with the context of infinite sequence. Similarly, MODWT is implemented as 'translation invariant DWT' [15], [16] and 'time-invariant DWT' [17].

In order to reduce the memory consumption, the features are extracted from the detail coefficients of the WT decomposition instead of giving the raw data directly. In this paper, the traditional DWT and the modified DWT are integrated with the feature extraction [18], [19] of PQD signals which is followed by classification.

The accurate detection of the PQ disturbance is the important performance indices in power quality analysis. However, the most common automated classification models are based on the Artificial Neural Network (ANN) [20], [21], fuzzy and neuro-fuzzy systems [22], [23], [24]. But the main disadvantage of ANN based classifier is the requirement of retraining when a new phenomenon is added. Hence, in this paper, two classifiers such as, Multilayer perceptron (MLP) and the Hidden Markov Model (HMMs) have been implemented to classify the PQD signals in order to establish a comparative assessment of MODWT application in PQ environment.
This paper organized as follows. The Section 2 describes the theory of the Second Generation Wavelet Transform (MODWT) along with the Discrete Wavelet transform (DWT). The feature extraction processes are presented in the Section-III. Section-IV provides the brief theory about the classifiers. Similarly, the Section-V deals with the construction of PQ model as well as the effectiveness of MODWT and DWT in the localization of the PQ disturbances. The classification results are presented in the Section-VII. Finally, Section-VIII provides the concluding remark.

II. LOCALIZATION APPROACH

The basic block diagram of the classification of PQ signals which is preceded by decomposition and feature extraction. The detection of the PQ disturbance has been carried out with the help of DWT and the MODWT. These have been described briefly in this section while the feature extraction and classification are described in the subsequent sections.

A. Continuous Wavelet Transform

The wavelet transform represents the signal as a combination of the wavelets at different location (position or amplitude) and scales (duration or time). The continuous wavelet transform generally implements for the continuous time signal analysis. The surface of the wavelet coefficients has been obtained from the different values of the scaling and the translation factors.

Mathematically, for a signal $x(t)$, the continuous wavelet transform [25] is expressed as

$$CWT(a,b) = \frac{1}{\sqrt{a}} \int_{-\infty}^{\infty} x(t) g\left(\frac{t-b}{a}\right) dt \tag{1}$$

where $g(\cdot)$ is the mother wavelet. Similarly, a is the scale factor and b is the translation factor. Both a and b are varies in continuous manner in continuous wavelet transform. In order to remove the redundancy due to continuous coefficients, discrete Wavelet transform has been introduced which has been discussed in next subsequent subsection.

B. Discrete Wavelet Transform

The discrete wavelet transform (DWT) implements in order to decompose a discretized signal into different resolution levels. The DWT reduces the substantial redundancy of CWT. In the multiresolution analysis (MRA), the wavelet function generates the detail coefficients of the decomposed signal and the scaling function generates the approximation coefficients of the decomposed signal. The DWT can be expressed with g as the mother wavelet

$$DWT(m,k) = \frac{1}{\sqrt{a_0^m}} \sum_n x(n) g\left(\frac{k - nb_0 a_0^m}{a_0^m}\right) \tag{2}$$

where k is an integer. The scaling parameter and translation parameter a and b vary in the discrete manner. The time signal $S[n]$ decomposed in to detailed $d_1(n)$ and smoothed $c_1(n)$ employing high pass ($h(n)$) and low pass filters ($l(n)$). Thus the detail version contains high frequency components than the smooth version $c_1(n)$. Mathematically, they are specified [26] as

$$c_1(n) = \sum_k h(k-2n) c_0(k) \tag{3}$$

$$d_1(n) = \sum_k g(k-2n) c_0(k) \tag{4}$$

where $c_0(n)$ is the discretised time signal (sampled version of $S_0(n)$). The outputs of the two filters are down sampled by a factor of 2 in order to obtain the DWT coefficients. The output of the low pass filter is called the approximation coefficients and the output of the high pass filter is called as the detail coefficients. The approximation coefficients are further fed to the low pass and high pass filter and the process is repeated. The high pass and low pass filters are called as the 'Quadrature mirror filters' and are related by the equation

$$h[L-1-n] = (-1)^n l(n) \tag{5}$$

where, L is the length of filter. The basic block diagram of DWT is shown in Fig.1.

The implementation of DWT is restricted with the length of signals. Similarly, the coefficients are affected by the change of initial point. The MODWT has been implemented in order to overcome the sensitivity of DWT with the choice of starting point of a time series.

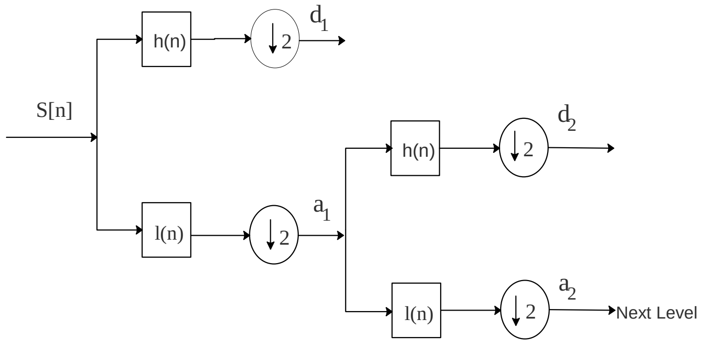

Fig. 1: Block diagram of DWT decomposition

C. Maximum Overlapping Discrete Wavelet Transform (MODWT)

The motivation to formulate the MODWT over the conventional DWT is the ability of the free selection of a starting point of a time series signal. The orthogonal transform of DWT suffers the lack of the invariance translation in time series analysis. The Maximum Overlap Discrete Wavelet Transform is the enhanced version of the Discrete Wavelet Transform (DWT). This transform can be employed to any sample size whereas the DWT is limited to the signal length N to be an intermultiple of 2^j where $j = 1,2,3,...,J$ is the scale number [27]. The representation of MODWT is shown in Fig.2. The MODWT scaling filters h_l and wavelet filters g_l are related to the DWT filters through (6) and (7)

$$\tilde{h}_l = \frac{h_l}{\sqrt{2}} \quad (6)$$

$$\tilde{g}_l = \frac{g_l}{\sqrt{2}} \quad (7)$$

The MODWT filters are also the Quadrature mirrors like DWT filters is given as (8) and (9)

$$\tilde{h}_l = (-1)^{l+1} h_{L-1-l} \quad (8)$$

$$\tilde{g}_l = (-1)^{l+1} g_{L-1-l} \quad (9)$$

where $l = 0,1,2,...,L-1$ and L is the width of the filter.

The n^{th} element of the first-stage wavelet and the scaling coefficients of MODWT with the input time series signal $X(n)$ is as follows

$$\widetilde{W}_{1,n} = \sum_{l=0}^{L_1-1} \tilde{h}_l X_{n-lmodN} \quad (10)$$

$$\widetilde{V}_{1,n} = \sum_{l=0}^{L_1-1} \tilde{g}_l X_{n-lmodN} \quad (11)$$

where $n = 1,2,3,...,N$ and N is the length of signal in sample.

$$\tilde{A}_{1,n} = \sum_{l=0}^{L_1-1} \tilde{g}_l \tilde{X}_{1,n+l \bmod N} \quad (12)$$

The first-stage approximations and details can be calculated by the equations (12) and (13). The MODWT scaling coefficients $\tilde{V}_j$ and $\tilde{W}_j$ wavelet coefficients at the n^{th} element of the j^{th} stage are given by the equations (14) and (15)

$$\widetilde{V}_{j,n} = \sum_{l=0}^{L_j-1} \tilde{g}_{j,1} \widetilde{X}_{n-lmodN} \quad (14)$$

$$\widetilde{W}_{j,n} = \sum_{l=0}^{L_j-1} \tilde{h}_{j,1} \widetilde{X}_{n-lmodN} \quad (15)$$

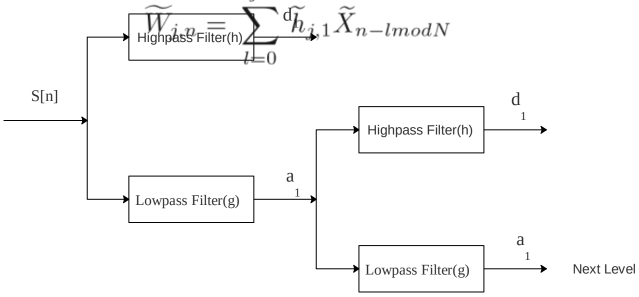

Fig. 2: Block diagram representation of MODWT decomposition

Similarly, the approximations A_j and the details D_j of the n^{th} element of the j^{th} stage MODWT are given by the equations (16) and (17).

$$\tilde{A}_{j,n} = \sum_{l=0}^{\tilde{L}_j-1} \tilde{g}_l^0 \tilde{V}_{1,n+l \bmod N} \tag{16}$$

$$\tilde{D}_{j,n} = \sum_{l=0}^{L_j-1} \tilde{h}_l^0 \tilde{W}_{1,n+l \bmod N} \tag{17}$$

Where $\tilde{g}_l^0$ is periodized g to length N and also the $\tilde{h}_l^0$ is periodized h to length N. So, the original time series signal can
be stated in terms of the approximations and the details as followse

$$X(n) = \sum_{l=0}^{j} \tilde{D}_j + \tilde{A}_j \tag{18}$$

III. THEORY OF THE FEATURE EXTRACTION

A. Feature extraction

The input to the classifiers has been extracted features from the output of the signal decomposition instead of directly using the raw data in ordered to reduce the computational burden. The quantitative analysis in terms of features like the energy content, the standard deviation (STD), the cumulative sum (CUSUM) and the entropy of the transformed signal has been performed to reduce the classification error. The basis of choosing the features has been explained below along with the proper expressions [28].

- **Energy** : According to Parseval's theorem the energy of the distorted signal will be partitioned at different resolution levels in different ways depending on the power quality disturbances signals. So, it has been established that energy distribution pattern changes when the amplitude and frequency of the signal changes [29] and [5].

  $$\text{Energy } ED_i = \frac{1}{N}\sum_{j=1}^{N} \left|D_{ij}\right|^2 \tag{19}$$

  where $i = 1,2,3,...,l$ (level of decomposition) and N is the number of samples in each decomposed data. D stands for detail coefficient.
- **Entropy** : The spectral entropy of the non-stationary power signal disturbances is an effective parameter for the classification of the signal. The entropy value for low frequency disturbances like the voltage swell, the voltage sag, the momentary interruption and the pure undistorted sinusoidal signal is minimum. The harmonics contained in the signals such as sag with harmonics, swell with harmonics have a comparatively high entropy value. For flicker type signals the entropy value is minimum. Similarly in case of the short duration non-stationary power signal disturbances such as the notches and the spikes have very low entropy values. While transients have relatively higher entropy value [8].

  $$\text{Entropy } ENT_i = -\sum_{j=1}^{N} D_{ij}^2 \log(D_{ij}^2) \tag{20}$$

- **Standard Deviation** : Assuming a zero mean, the standard deviation can be considered as a measure of the energy of the considered signal. Standard deviation has been employed to differentiate the low frequency and the high frequency signals [5].

  $$\text{Standard Deviation } \sigma_i = \left(\frac{1}{N}\sum_{j=1}^{N}(D_{ij} - \mu_i)^2\right)^{\frac{1}{2}} \tag{21}$$

- **CUSUM** : The cumulative sum method implements the samples for the localization of the distortion in the signal. The CUSUM has been computed by the sum of the consecutive samples of the power quality signal after being passed through the aforementioned transforms [30].

$$\text{CUSUM} \quad CM_i = \sum_{j=1}^{N} (D_{ij} - \mu_i)^2$$

(22)

where Mean $\mu_i = \frac{1}{N} \sum_{j=1}^{N} D_{ij}$

These four features have been extracted from the output of the transformation. At each level four features have been extracted, so for each signal in WT 4 ∗ 7 feature vector have been formed. After calculating the features for the complete data sets, the feature vectors are normalised between [0,1] by considering the maximum value of the corresponding feature vectors as the base. However, the normalisation is one of the important steps of pre-processing of the data before classification. This vector normalisation has been carried out in order to avoid the influence of high range feature vectors over low range ones. The extracted features have been fed as put to the classifiers.

IV. CLASSIFICATION APPROACH

The extracted features are fed as inputs to the classifier such as MLP and HMMs.

A. Hidden Markov models (HMMs)

The HMMs have been applied to feature vector extracted from the coefficient in order to determine the maximum likelihood in the data set. The HMM, extension of the Markov model in which the stochastic process is not directly observable through another set of stochastic processes. However, an HMM can be defined as $\lambda = (M,N,\pi,A,B)$ where the parameter N denotes the number of states of the model, M is the number of distinct observation symbols per state, π is the initial state distribution vector, similarly , A denotes the state transition probability and finally B is observation probability matrices respectively. A discrete HMM is explained in [25], [8] through the model of individual states.

Like other classifiers, the HMMs operation has been partitioned into the training and the testing stage of dataset. The HMM training model uses both continuous and discrete density modelling and also employs the Baum-Welch algorithm to construct the HMMs [31]. Starting with a very simple prototype system, the HMMs are repeatedly modified and re-estimated until the required level of model complexity and performance is reached. In this study, ten different HMMs has been trained for ten different disturbance classes. For this classification process, the logarithmic probability of each model output has been determined for the unknown input signals. In order to develop a proper HMM, the selection of the optimum number of state and the density function are very important but there is no explicit rule for the selection of these factors except the application type and the parameters. In this work, three states has been selected to stipulate the output with the Gaussian mixtures function. The prior distribution has been used over the state transition to favour the transitions in order to stay in the same state. The prior is multiplied by the likelihood function and then normalised according to the Bayes theorem. The CA depends on the number of matching of the testing with the trained model using the equation.

V. POWER QUALITY DISTURBANCE MODEL

The theory described in Section-II has been used to compute the approximation and detail coefficients up to fourth finer levels using the DWT and MODWT. The PQD signals are simulated in MATLAB with sampling frequency is 3.2 kHz. Class labels assigned to PQ signals of synthesized signals are given in Table I.

TABLE I: Power signal Class labels of synthesis signal

PQD events	Class
Sag	*CL*1
Swell	*CL*2
Interruption	*CL*3
Oscillatory transient	*CL*4
Flicker	*CL*5
Harmonics	*CL*6
Sag + Harmonics	*CL*7
Swell + Harmonics	*CL*8
Notch	*CL*9
Spike	*CL*10

VI. DECOMPOSITION OF PQ SIGNALS

A. Pure Sinusoidal Voltage Signal

A pure sinusoidal wave of voltage signal is considered in Fig.3. With DWT and MODWT, the signal has been decomposed up to four decomposition levels are shown in Fig.3 along with the original sine wave. The the vertical axis represents the amplitude of voltage signal in volt V p.u. (per unit) and similarly the horizontal axis presents the time (in second) in terms of samples. Both DWT and MODWT has been implemented on the aforementioned PQ signals in order to carry out the analysis.

By decomposing normal voltage, similar types of waveforms are produced at the respective decomposition level both in DWT and the MODWT present in Fig. 3 along with the original waveform. In MODWT, the initial point is shifted due to circular shifting which helps in future prediction. The decomposition levels and the corresponding description of the pure sine wave with sag and swell are shown in Fig. 4 and Fig. 5 respectively.

B. Pure sine wave with sag

Pure sine wave with sag has been considered for analysis. In Fig. 4, sag detection can be observed at levels 1,2,3 and 4. In DWT decomposition, the starting and the end point of the distortion of each decomposition level are in same alignment with the original signal, however in MODWT decomposition the first decomposed level is at the alignment with the original signal but the others are shifted due to the circular shifting.

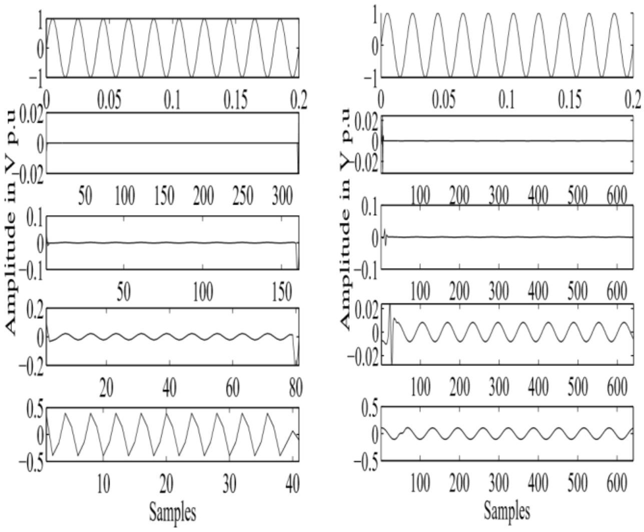

From the Fig. 4, it is observed that, both the DWT and the MODWT decomposition provided similar type of waveforms along with the shifting.

C. Pure sine wave with swell

The procedure adopted for this type of signal is the same as the previous case. In Fig. 5, similar types of waveforms have been found in the same decomposition levels.

Similarly, the rest PQ disturbances are subjected to the process of decomposition using the DWT and the MODWT. Similar types of waveforms has been also obtained from both the types of the wavelet transforms.

In decomposition levels other than the 1st, the initial point of the signal is also sifted along with the distortions. So, MODWT can be implemented to predict the occurrence of power quality distortions.

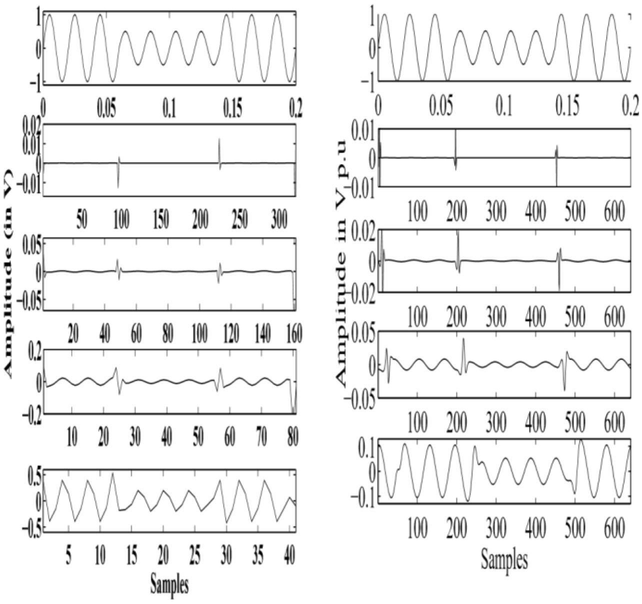

(a) (b)

Fig. 3: Localization of pure sine wave in (a) DWT decomposition (b) MODWT decomposition

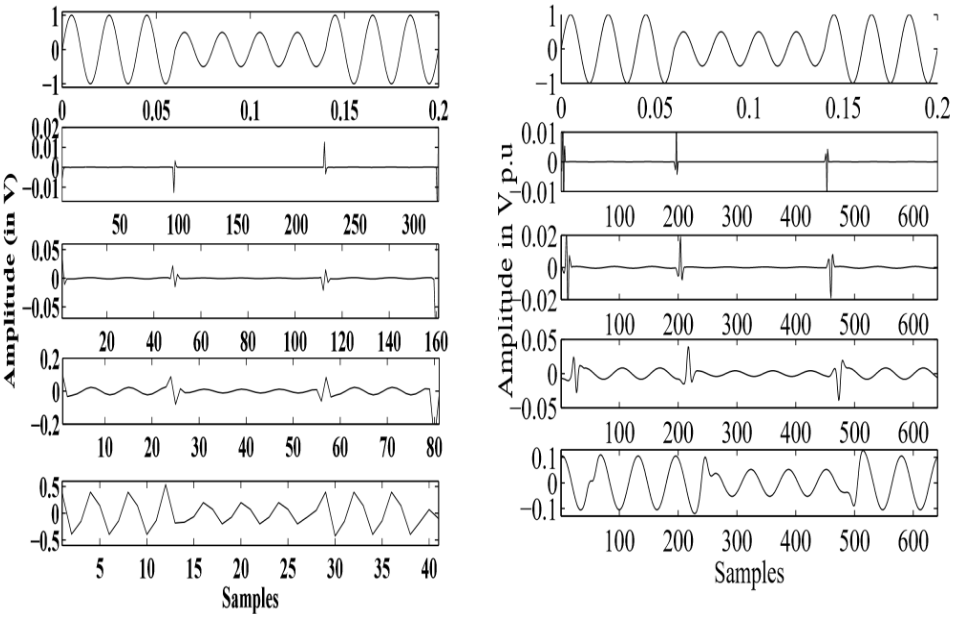

(a) (b)

Fig. 4: Localization of sine wave with sag in (a) DWT decomposition (b) MODWT decomposition

D. Harmonic voltage signal

Consider the harmonic signal shown in Fig. 6. By observing 1^{st} two levels of Fig. 3 and Fig. 6, it can be observed that for sinusoidal signal the magnitude of 1^{st} two levels are almost zero and for harmonic signal, 1^{st} two levels have some magnitude. Hence, it can be concluded that the waveforms of each level are different for different disturbance and this property helps in classification of those disturbances.

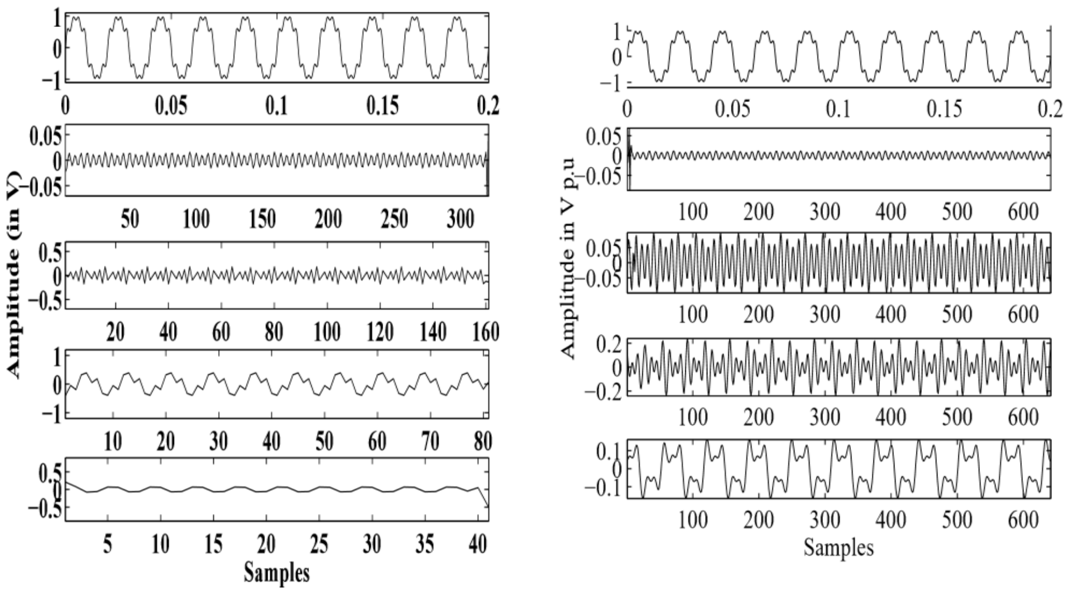

(a) (b)

Fig. 5: Localization of sine wave with swell in (a) DWT decomposition (b) MODWT decomposition

E. Pure sine wave with Harmonic and sag

A pure sine wave voltage signal with harmonic and sag has been considered for analysis in Fig. 7. Similar type of wave form have been found.

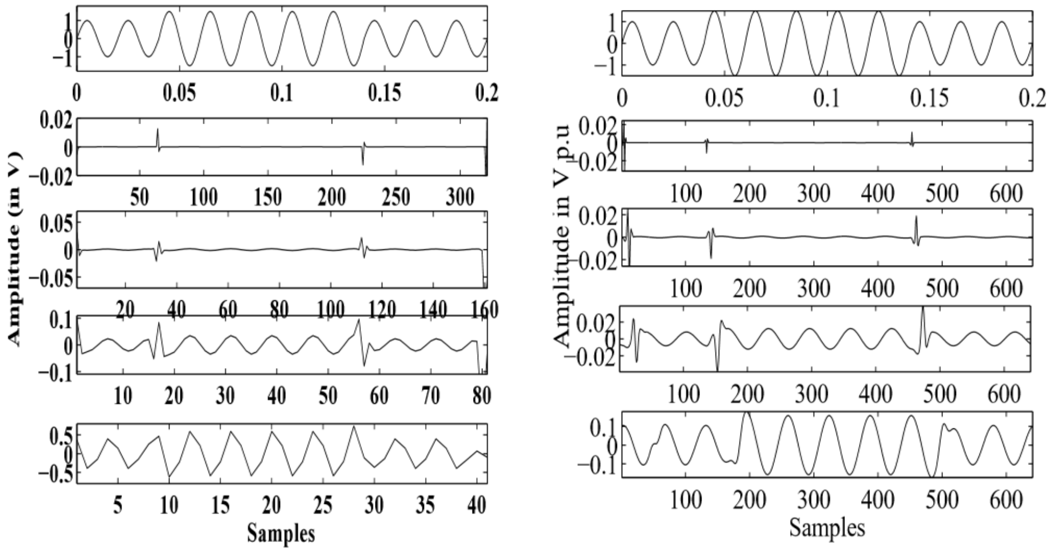

(a) (b)

Fig. 6: Sine wave with Harmonic (a) DWT decomposition (b) MODWT decomposition

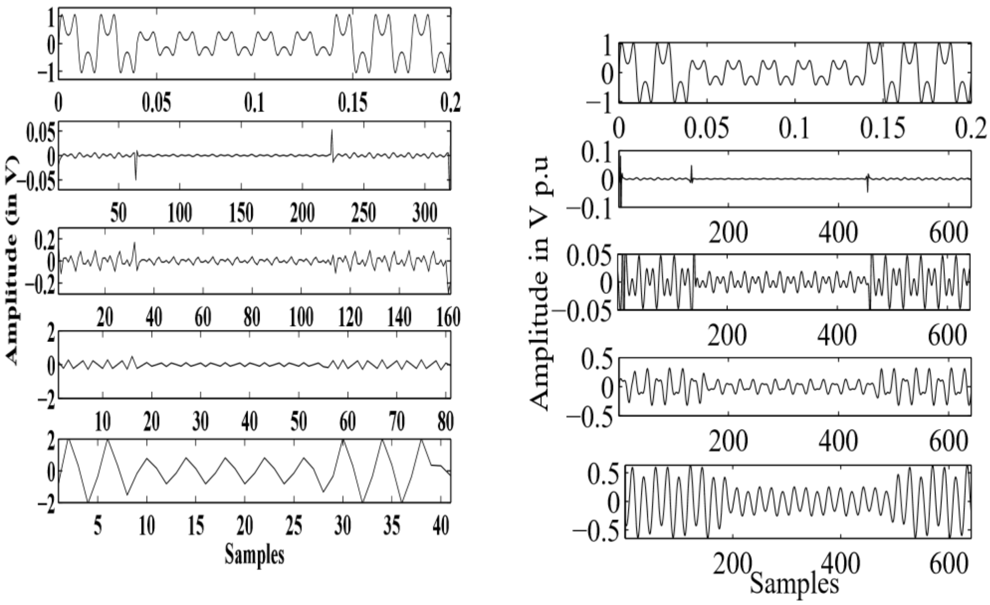

(a) (b)

Fig. 7: Sine wave with Harmonic and sag (a) DWT decomposition (b) MODWT decomposition

Similar to that of other cases, the origin point of signals shifted along with the distortion in the decomposition levels

MODWT.

F. Experimental PQD Signal generation

In order to get the real data, seven types of PQ signals have been generated by employing transmission line panel, the load and the storage oscilloscope. The transmission demo panel comprises a line model with the length 400 Km and voltage of 220 kV. The lumped parameter line model with five cascaded networks each of them has been designed for 80 km parameters. The fault simulating switch has been provided to create the fault condition. This transmission line panel also comprises digital DSP based power analyzers, voltmeters, ammeters, push buttons, indicating lamp and accessories. A digital timer is also present. The demo panel is also provided with protective devices i.e MCB'S to give protection from any abnormal condition occurring

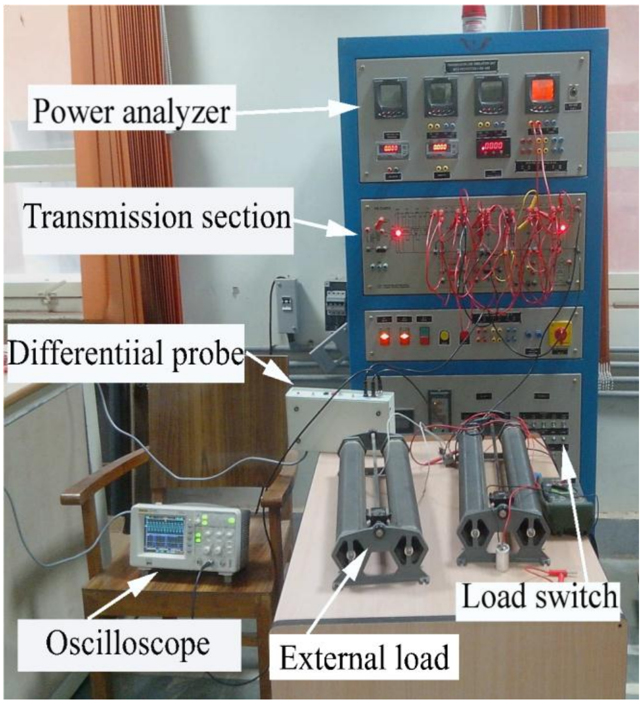

Fig. 8: Experimental setup for single phase voltage signal collection

during the actual demonstration and experiments. The numerical impedance relay and the numerical over current relay are also associated to give trip signal to the circuit breaker. The current carrying capacity of the model is 5 Amp.

The seven types of signals are sag, swell, interruption, sag with swell, sag with interruption, swell with interruption and sag and swell with interruption. A 220 V is applied to the transmission line panel and by changing the load and creating fault, the various disturbances are created. The disturbances are then stored in storage oscilloscope. Then data is extracted from the oscilloscope and fed to the MATLAB for feature extraction and subsequent classification. The details of experimental set up is given in Fig. 8. Similarly, the circuit diagram of the transmission panel has been shown in Fig. 9. The captured single phase voltage signals with sag, swell and interruption are presented in Fig. 10.

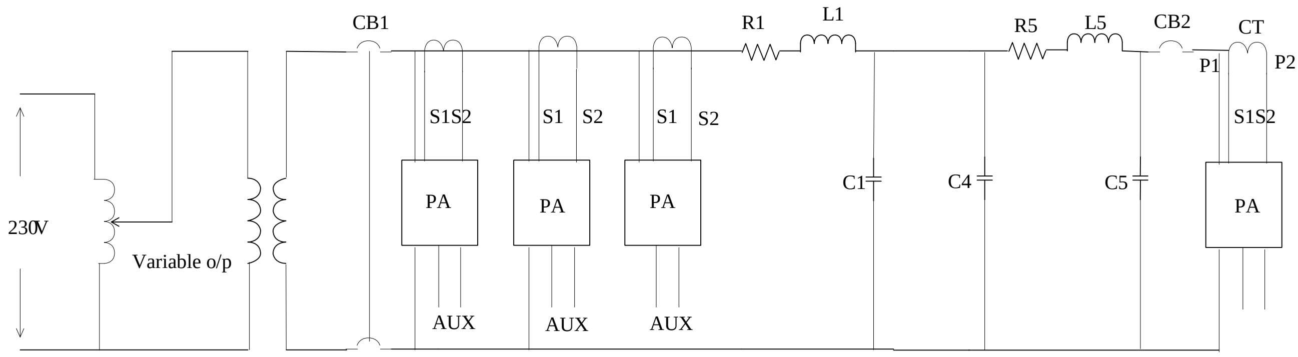

Fig. 9: Circuit diagram of the single phase transmission panel connection

VII. CLASSIFICATION RESULTS

A. Classification with simulated PQD signals

The classification accuracy is computed by the automated classifiers described in Section-III. The total 10936 numbers PQD signals are simulated with MATLAB. Each data set contains variable X ($X1$– standard deviation, $X2$– energy of details, $X3$– entropy, $X3$– $X3$–) and L($L1$,$L2$,...,$L7$ level of decomposition) which constitute 28 features. For each classifier 70% of the total data has been treated as the training data and the rest 30% data are employing for the testing.

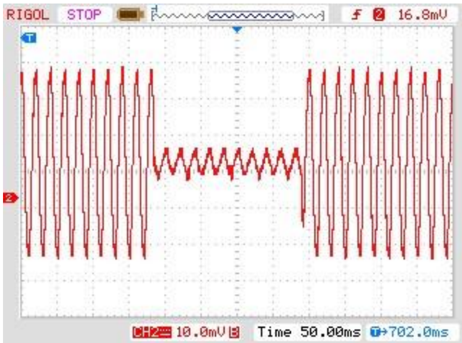

(a) Voltage with sag

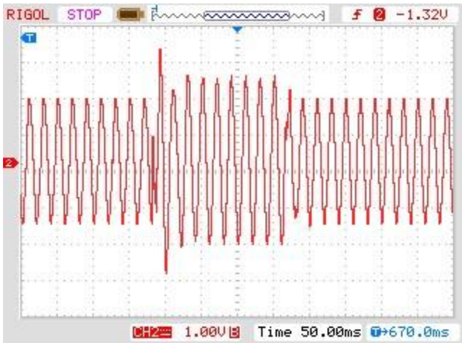

(b) Voltage with swell

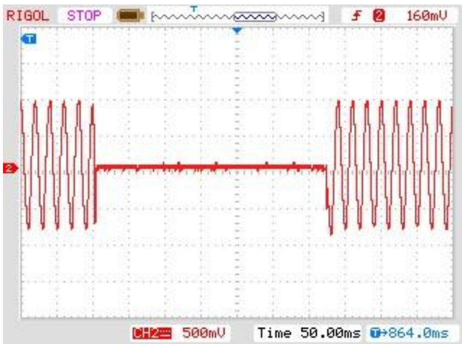

(c) Voltage with interruption

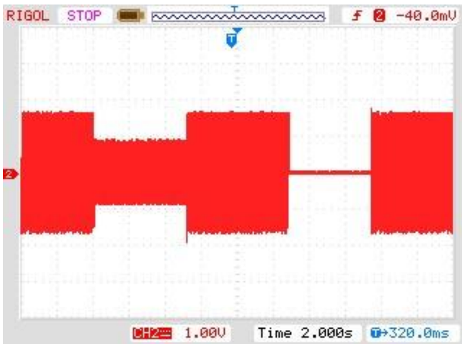

(d) Voltage with interruption and sag

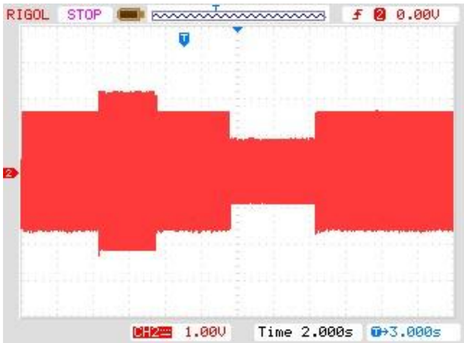

(e) Voltage with sag and swell

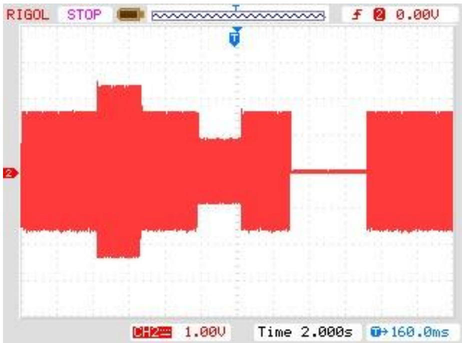

(f) Voltage with sag, swell and interruption

Fig. 10: Single phase real voltage signals with disturbances

For ten different types of disturbances the overall classification accuracy (%CA) is also calculated individually. The classification accuracy is a measure of the performance index of the PQ defined [32] as

$$Classification\ Accuracy(\%) = \frac{Number\ of\ samples\ correctly\ classified}{Tota\ number\ of\ samples\ in\ the\ class} \times 100 \tag{23}$$

In the Table II, the (CA%) of MLP and HMMs classifiers also have been presented. From, Table II, it has been observed that for each data set the overall (CA%) of MLP is better than the HHMs as HHMs fail to classify interruption, harmonic like slow disturbances. Moreover, from the individual (CA%), it can be observed, the HMMs has better (CA%) than the MLP in case of fast signals like transient, notch and spike etc.

TABLE II: CA (%) of Pure Signals

CLASS	DWT		SGWT	
	MLP	HMMs	MLP	HMMs
CL1	86.56	76.21	87.57	77.09
CL2	86.96	98.32	87.12	98.34
CL3	90.01	0	90.78	0
CL4	89.94	98.01	90.03	98.45
CL5	87.79	92.01	88.02	93.12
CL6	91.11	47.61	92.13	48.63
CL7	87.34	43.32	88.09	44.78
CL8	88.47	73.60	89.91	74.37
CL9	90.34	100	90.78	100
CL10	89.07	98.02	90.65	98.45
TOTAL %CA	89.82	71.02	90.50	72.32

The classification of three phase PQ disturbances have been presented in Table III. From Table III, it can be observed that %CA value of three phase signals are similar to the synthetic signal %CA value. TABLE II: CA (%) of Pure Synthesized Signals

TABLE III: CA (%) of real time single phase signals

CLASS	DWT		MODWT	
	MLP	HMMs	MLP	HMMs
C1	82.56	72.36	83.50	72.72
C2	83.36	92.47	84.21	93.07
C3	87.21	0	87.79	0
C1+C2	85.34	88.34	85.83	91.32
C1+C3	84.39	13.01	84.93	90.07
C2+C3	83.16	47.61	83.19	47.92
C1+C2 +C3	84.34	43.32	85.02	33.45
TOTAL %CA	84.21	60.34	85.75	62.02

B. Fault Classification

Under normal operating condition, the power system operates under balanced conditions with all the equipments carrying normal currents and voltages within the prescribed limits. This healthy operating condition can be disrupted due to a fault in the system. The power system faults are divided in to three phase balanced fault and unbalanced fault. The different types of unbalanced fault are single line to ground fault (L–G), line to line fault (L–L), double line to ground (L–L–G). The balanced faults are three phase fault which are severe type of fault. These faults can be two types such as line to line to line to ground (L–L–L–G) and line to line to line fault (L–L–L).

Three phase voltage signals with fault are captured from an overhead π modelled transmission line of length 360 (Km) like the other cases. Total five types of fault signals are captured. Some of fault signals have been presented in Fig.11. Fault signals have been captured from the oscilloscope and fed to MATLAB for analysis like the previous cases. From the details of the WT and the ST contours four features have been extracted and fed to the classifiers in order to recognise the type of fault. The recognition rate in terms of %*CA* is given in Table IV. Different approaches have been implemented for calculation of %*CA* in Table IV. From these tables, it can be observed that all these proposed techniques are working satisfactorily. The HMM has provided good results unlike the PQ disturbance recognition where it failed to recognise slow disturbances perfectly.

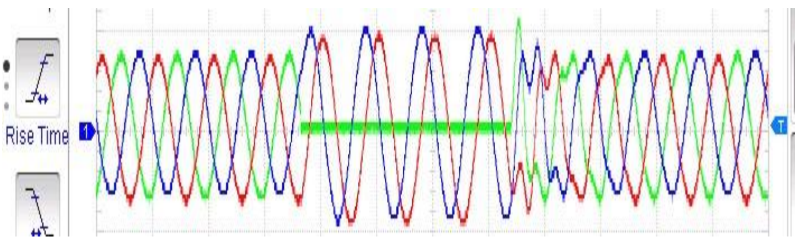

(a) L–G fault

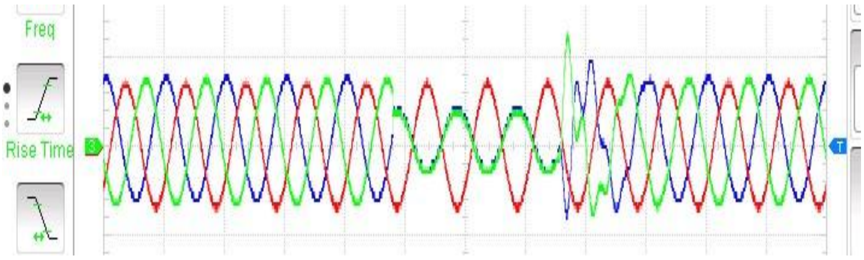

(b) L–L fault

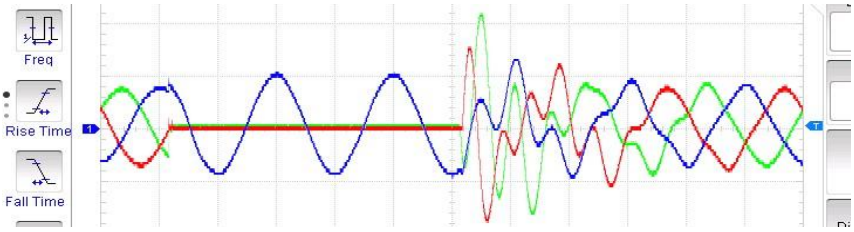

(c) L-L-G fault

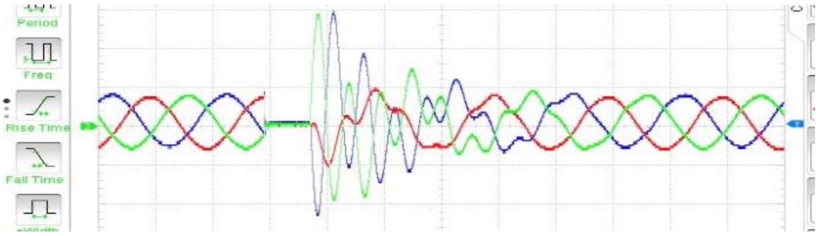

(d) L-L-L-G fault

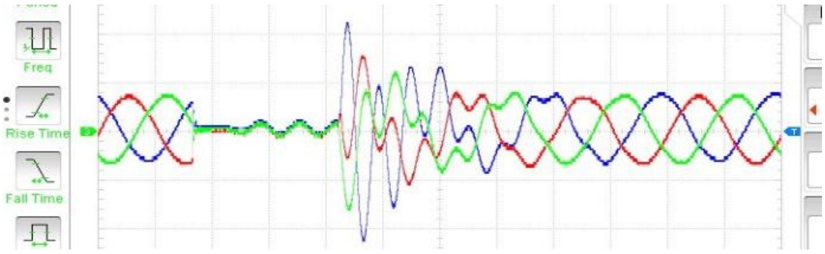

(e) L-L-L fault

Fig. 11: Three phase real voltage signals fault

TABLE IV: CA (%) of three phase fault signals

CLASS	DWT		MODWT	
	MLP	HMMs	MLP	HMMs
L-G	75.21	80.0	82.00	80.71
L-L	83.76	78.76	82.01	83.52
L-L _G	86.75	88.33	81.82	85.70
L–L– L-G	74.14	81.17	85.33	91.58
L–L –L	91.42	91.94	88.63	82.41
TOTAL %CA	83.51	85.42	87.35	87.96

VIII. CONCLUSION

The useful features of the PQD signals have been extracted from the DWT and the MODWT decomposition. The classification accuracy of these simulated and the three phase real signals are obtained by MODWT and DWT with the combination of automatic classifiers such as HMMs, DT and RF. From these aforementioned classifiers, it is observed that although DWT has yielded similar classification accuracy like the MODWT. The down sampling free MODWT provides the proper localization of PQ disturbances along with the shifting. Elimination of down sampling overcomes the restriction in the choice of signal length. The insensitivity to the choice of starting point of time series has made MODWT as a suitable technique in real time environment. The HHMs have classified the fast signals successfully. In case of fault recognition, HMMs have provided good result. Moreover, the HMMs also perform satisfactorily on real time environment.

IX. REFERENCES

[1] M. Bollen, “What is power quality?,” *Electric Power Systems Research*, vol. 66, no. 1, pp. 5–14, 2003.

[2] P. Janik and T. Lobos, “Automated classification of power-quality disturbances using svm and rbf networks,” *IEEE Transactions on Power Delivery*, vol. 21, no. 3, pp. 1663–1669, 2006.

[3] S. Khokhar, A. Mohd Zin, A. Mokhtar, and N. Ismail, “Matlab/simulink based modeling and simulation of power quality disturbances,” in *IEEE Conference on Energy Conversion (CENCON)*, pp. 445–450, IEEE, 2014.

[4] D. O. Koval, “Power system disturbance patterns,” *IEEE Transactions on Industry Applications*, vol. 26, no. 3, pp. 556–562, 1990.

[5] A. Gaouda, M. Salama, M. Sultan, and A. Chikhani, “Power quality detection and classification using wavelet-multiresolution signal decomposition,” *IEEE Transactions on Power Delivery*, vol. 14, no. 4, pp. 1469–1476, 1999.

[6] L. Angrisani, P. Daponte, M. D’apuzzo, and A. Testa, “A measurement method based on the wavelet transform for power quality analysis,” *Power Delivery, IEEE Transactions on*, vol. 13, no. 4, pp. 990–998, 1998.

[7] D. Gabor, “Theory of communication. part 1: The analysis of information,” *Journal of the Institution of Electrical Engineers-Part III: Radio and Communication Engineering*, vol. 93, no. 26, pp. 429–441, 1946.

[8] B. Biswal, M. Biswal, S. Mishra, and R. Jalaja, “Automatic classification of power quality events using balanced neural tree,” *Industrial Electronics, IEEE Transactions on*, vol. 61, no. 1, pp. 521–530, 2014.

[9] R. A. Brown and R. Frayne, “A fast discrete s-transform for biomedical signal processing,” in *Engineering in Medicine and Biology Society, 2008. EMBS 2008. 30th Annual International Conference of the IEEE*, pp. 2586–2589, IEEE, 2008.

[10] I. Daubechies, “Orthonormal bases of compactly supported wavelets,” *Communications on pure and applied mathematics*, vol. 41, no. 7, pp. 909–996, 1988.

[11] A. G. Hafez, E. Ghamry, H. Yayama, and K. Yumoto, “A wavelet spectral analysis technique for automatic detection of geomagnetic sudden commencements,” *Geoscience and Remote Sensing, IEEE Transactions on*, vol. 50, no. 11, pp. 4503–4512, 2012.

[12] D. B. Percival and A. T. Walden, “Wavelet methods for time series analysis (cambridge series in statistical and probabilistic mathematics),” 2000.

[13] M. J. Shensa, “The discrete wavelet transform: wedding the a trous and mallat algorithms,” *Signal Processing, IEEE Transactions on*, vol. 40, no. 10, pp. 2464–2482, 1992.

[14] G. P. Nason and B. W. Silverman, “The stationary wavelet transform and some statistical applications,” *LECTURE NOTES IN STATISTICS-NEW YORK-SPRINGER VERLAG-*, pp. 281–281, 1995.

[15] R. Coifman and D. Donoho, "Translation-invariant de-noising, in wavelets and statistics(a. antoniadis, ed.)," 1995.

[16] R. Coifman and D. Donoho, "Translation-invariant de-noising, in wavelets and statistics(a. antoniadis, ed.)," 1995.

[17] J.-C. Pesquet, H. Krim, and H. Carfantan, "Time-invariant orthonormal wavelet representations," *Signal Processing, IEEE Transactions on*, vol. 44, no. 8, pp. 1964–1970, 1996.

[18] C.-Y. Lee and Y.-X. Shen, "Optimal feature selection for power-quality disturbances classification," *Power Delivery, IEEE Transactions on*, vol. 26, no. 4, pp. 2342–2351, 2011.

[19] B. Panigrahi and V. R. Pandi, "Optimal feature selection for classification of power quality disturbances using wavelet packet-based fuzzy k-nearest neighbour algorithm," *IET generation, transmission & distribution*, vol. 3, no. 3, pp. 296–306, 2009.

[20] A. S. Yilmaz, A. Subasi, M. Bayrak, V. M. Karsli, and E. Ercelebi, "Application of lifting based wavelet transforms to characterize power quality events," *Energy conversion and management*, vol. 48, no. 1, pp. 112–123, 2007.

[21] A. K. Ghosh and D. L. Lubkeman, "The classification of power system disturbance waveforms using a neural network approach," *Power Delivery, IEEE Transactions on*, vol. 10, no. 1, pp. 109–115, 1995.

[22] S. Hasheminejad, S. Esmaeili, and S. Jazebi, "Power quality disturbance classification using s-transform and hidden markov model," *Electric Power Components and Systems*, vol. 40, no. 10, pp. 1160–1182, 2012.

[23] M. B. I. Reaz, F. Choong, M. S. Sulaiman, F. Mohd-Yasin, and M. Kamada, "Expert system for power quality disturbance classifier," *Power Delivery, IEEE Transactions on*, vol. 22, no. 3, pp. 1979–1988, 2007.

[24] S. Mishra, C. Bhende, and B. Panigrahi, "Detection and classification of power quality disturbances using s-transform and probabilistic neural network," *Power Delivery, IEEE Transactions on*, vol. 23, no. 1, pp. 280–287, 2008.

[25] S. Santoso, E. J. Powers, W. M. Grady, and P. Hofmann, "Power quality assessment via wavelet transform analysis," *Power Delivery, IEEE Transactions on*, vol. 11, no. 2, pp. 924–930, 1996.

[26] C. H. Kim and R. Aggarwal, "Wavelet transforms in power systems. i. general introduction to the wavelet transforms," *Power Engineering Journal*, vol. 14, no. 2, pp. 81–87, 2000.

[27] D. B. Percival and A. T. Walden, *Wavelet methods for time series analysis*, vol. 4. Cambridge University Press, 2006.

[28] B. Panigrahi and V. R. Pandi, "Optimal feature selection for classification of power quality disturbances using wavelet packet-based fuzzy k-nearest neighbour algorithm," *IET generation, transmission & distribution*, vol. 3, no. 3, pp. 296–306, 2009.

[29] T. Zhu, S. Tso, and K. Lo, "Wavelet-based fuzzy reasoning approach to power-quality disturbance recognition," *Power Delivery, IEEE Transactions on*, vol. 19, no. 4, pp. 1928–1935, 2004.

[30] S. Mohanty, A. Pradhan, and A. Routray, "A cumulative sum-based fault detector for power system relaying application," *IEEE Transactions on Power Delivery*, vol. 23, no. 1, pp. 79–86, 2008.

[31] L. R. Rabiner, "A tutorial on hidden markov models and selected applications in speech recognition," *Proceedings of the IEEE*, vol. 77, no. 2, pp. 257–286, 1989.

[32] M. Biswal and P. K. Dash, "Measurement and classification of simultaneous power signal patterns with an s-transform variant and fuzzy decision tree," *Industrial Informatics, IEEE Transactions on*, vol. 9, no. 4, pp. 1819–1827, 2013.